Available online at www.sciencedirect.com
SCIENCE DIRECT®
ELSEVIER
European Journal of Mechanics B/Fluids 23 (2004) 491–500
EUROPEAN JOURNAL OF MECHANICS B/FLUIDS

Sound generation by turbulence

A.P. Dowling, T.P. Hynes

Department of Engineering, University of Cambridge, Trumpington Street, Cambridge, CB2 1PZ, UK

Received 23 June 2003; received in revised form 21 August 2003; accepted 30 October 2003

Abstract

Sound is a weak by-product of a subsonic turbulent flow. The main convective elements of the turbulence are silent and it is only spectral components with supersonic phase speeds that couple to the far-field sound. This paper reviews recent work on sound generation by turbulence. Just as there is a hierarchy of numerical models for turbulence (scaling, RANS, LES and DNS), there are different approaches for relating the near-field turbulence to the far-field sound. Kirchhoff approaches give the far-field sound in a straightforward way, but provide little insight into the sources of sound. Acoustic analogies can be used with different base flows to describe the propagation effects and to highlight the major noise producing regions.

1. Introduction

Sound generation by turbulence in the propulsive jet is a major element of an aircraft's noise at take-off and needs to be reduced if society's demands for quieter aircraft are to be met. This is challenging because turbulence is remarkably inefficient as an acoustic source. In the absence of any solid surfaces, the turbulent Reynolds stresses form quadrupole acoustic sources with significant cancellation in the way they generate sound [1]. Investigation of the characteristics of sound generation and propagation from quadrupole sources, together with estimates of the typical order of magnitudes of the turbulent stresses and their integral length scales, led to Lighthill's celebrated eighth-power law. This law states that the radiated sound power from a cold subsonic jet increases in proportion to the eighth-power of the jet velocity, but with only the square of the jet diameter. There is then significant noise reduction if the jet diameter is increased, and the velocity decreased, while maintaining the same thrust. This has been used with great effect in aeroengines over the last forty years: bypass ratios have increased, with the thrust being generated by moving a greater mass of air more slowly, leading to a reduction in the radiated sound at fixed thrust. However, now aeroengines have evolved to be as large as possible (at least if they are to fit underneath a conventional aircraft wing!!) and jet noise is still the dominant noise mechanism at takeoff. More subtle modifications are needed, and manufacturers are willing to make such modifications – even if they increase the drag slightly.

The development of new devices to reduce the sound involves a delicate balance. While jets in unbounded space are inefficient, the radiated sound can increase dramatically when surfaces are introduced. However, the most straightforward way of modifying the characteristics of the turbulence is through the introduction of additional surfaces such as, for example, small protuberances into the jet or nozzle-lip serrations or crenellations which enhance mixing [2]. The optimisation of such devices is challenging: they have a drag penalty which must be minimised; and even when the generated sound power is reduced at some frequencies it may be increased at others [3]. However, if the increase is modest and occurs at high enough frequencies, there may be a worthwhile net reduction in the sound heard by a listener on the ground, simply because high-frequency sound is attenuated more effectively by propagation through the atmosphere. There are currently no models that can be used reliably to assess the effectiveness of jet noise reduction devices and their design is almost entirely empirical. The development of appropriate analytical and computational tools requires the integration of ideas from turbulence modelling and acoustics.

E-mail addresses: apd1@eng.cam.ac.uk (A.P. Dowling), tph@eng.cam.ac.uk (T.P. Hynes).

0997-7546/$ – see front matter
doi:10.1016/j.euromechflu.2003.10.014

This paper reviews recent work in aeroacoustics. The scales in a turbulent jet give an indication of the inherent challenges. The Reynolds numbers of interest are high, typically in the range $10^5 \to 10^7$ in practical applications. This means that of the order of $10^{12} \to 10^{15}$ grid points are needed to resolve all relevant turbulence scales. Even if models are used for the sub-grid turbulence, the geometrical scales still span a large range: much of the high frequency sound is generated near the jet lip, where the shear layers are very thin, typically less than $0.05D$, where D is the jet diameter, whereas the peak noise production is near the end of the potential core, some 7 jet diameters further downstream. We are interested in the noise radiated to the far field and that means distances much larger than the extent of the source region requiring radial distances r greater than $40D$. For a direct numerical calculation, at least 6–8 mesh points/wavelength are needed. Moreover, a broad frequency range is of interest, 100 Hz–10 kHz, which corresponds to Strouhal numbers based on jet exit velocity in the range $0.01 < fD/U_j < 1.0$ for a typical jet.

The jet is inefficient as an acoustic source: typically the sound power will be between 10^{-5} and 10^{-4} of the jet power, with $u'_{\text{acoustic}} \sim 10^{-4} u'_{\text{jet}}$ and so any numerical code used to predict the noise of turbulence needs be highly accurate if it is not to introduce spurious sources of this order due to digitisation errors. Neither should the code introduce any significant numerical dissipation or dispersion. Moreover, it is essential to have non-reflecting boundary conditions and to enable the jet to exit the computational domain silently [4,5]. All these are stringent demands.

The numerical difficulties arise because of the low efficiency of turbulent sources and this low efficiency is because most of a turbulent flow is silent. The challenge is to capture the weak source producing elements in the turbulence, in the presence of the much more intense hydrodynamic fluctuations. Any modelling scheme or experimental investigation must be developed with a firm view of what components of a turbulent flow actually generate acoustic waves and we discuss the sources of sound in Section 2.

Effective modelling of sound generation by turbulence requires the coupled consideration of the propagation of acoustic waves through the jet or wall boundary layer to the acoustic far field, together with an assessment of the turbulent sources. Just as there is a hierarchy of different approaches for turbulence modelling (scaling, RANS, LES and DNS), different techniques and levels of approximation have been applied to this radiation problem. The advantages and disadvantages of the various methods are reviewed in Section 3. There is no universal 'best' method – indeed the choice depends not only on the form of the information available on the near-field flow, but also on how the resulting far-field sound will be used: whether the requirement is just for a predicted sound pressure level, or whether the method should enhance understanding of what, and where in the jet, are the main noise sources.

2. Turbulence as a source of sound

A turbulent flow may have very energetic velocity fluctuations, with significant pressure fluctuations, but only certain components of this energetic flow generate acoustic waves that propagate to the far field with the speed of sound. Lighthill's acoustic analogy provides a very convenient mechanism to investigate how turbulence generates sound. Lighthill [1] rearranged the Navier–Stokes equation into the form of an inhomogeneous wave equation:

$$\frac{\partial^2 \rho'}{\partial t^2} - c_0^2 \nabla^2 \rho' = \frac{\partial^2 T_{ij}}{\partial x_i \partial x_j}, \tag{1}$$

ρ is the density perturbation, p the pressure and c the speed of sound. T_{ij} is Lighthill's quadrupole, $T_{ij} = \rho u_i u_j + (p' - c_0^2 \rho')\delta_{ij} - \sigma_{ij}$, where in an isothermal jet the main contribution is from the unsteady Reynolds stresses. The prime denotes a perturbation and the suffix zero the mean value in the distant field.

The solution to this inhomogeneous equation is

$$\rho'(\mathbf{x}, t) = \frac{\partial^2}{\partial x_i \partial x_j} \int \frac{T_{ij}(\mathbf{y}, t - |\mathbf{x} - \mathbf{y}|/c_0)}{4\pi c_0^2 |\mathbf{x} - \mathbf{y}|} \, \mathrm{d}^3\mathbf{y}, \tag{2}$$

which in the far-field simplifies to

$$p'(\mathbf{x}, t) = \frac{x_i x_j}{4\pi c_0^2 |\mathbf{x}|^3} \frac{\partial^2}{\partial t^2} \int T_{ij}\left(\mathbf{y}, t - \frac{|\mathbf{x}|}{c_0} + \frac{\mathbf{x} \cdot \mathbf{y}}{|\mathbf{x}| c_0}\right) \mathrm{d}^3\mathbf{y}. \tag{3}$$

This relates the radiated sound pressure at an observer's position $\mathbf{x}$ at time t to an integral over the source region of the quadrupole T_{ij} evaluated at a time earlier than t by the time taken for the sound to travel from the source position $\mathbf{y}$ to $\mathbf{x}$.

Only elements of the turbulence that contribute to this volume integral influence the far-field sound. We can identify these components by investigating disturbances of frequency ω. Taking the Fourier transform in time of Eq. (3) leads to

$$\hat{p}(\mathbf{x},\omega) = -\frac{\omega^2 x_i x_j \, \mathrm{e}^{-\mathrm{i}\omega|\mathbf{x}|/c_0}}{4\pi c_0^2 |\mathbf{x}|^3} \int \widehat{T}_{ij}(\mathbf{y},\omega)\, \mathrm{e}^{\mathrm{i}\omega \mathbf{x}\cdot\mathbf{y}/(|\mathbf{x}|c_0)}\, \mathrm{d}^3\mathbf{y}, \tag{4}$$

where the circumflex denotes the Fourier component. The volume integral can now be evaluated in terms of $\widetilde{T}_{ij}(\mathbf{k},\omega)$, the wavenumber-frequency decomposition of T_{ij}, which is defined as

$$\widetilde{T}_{ij}(\mathbf{k},\omega) = \int T_{ij}(\mathbf{y},\tau)\, \mathrm{e}^{-\mathrm{i}(\omega\tau+\mathbf{k}\cdot\mathbf{y})}\, \mathrm{d}^3\mathbf{y}\, \mathrm{d}\tau = \int \widehat{T}_{ij}(\mathbf{y},\omega)\, \mathrm{e}^{-\mathrm{i}\mathbf{k}\cdot\mathbf{y}}\, \mathrm{d}^3\mathbf{y}.$$

The volume integral in Eq. (4) is simply $\widetilde{T}_{ij}(\mathbf{k},\omega)$ with $\mathbf{k} = -\omega\mathbf{x}/c_0|\mathbf{x}|$, giving

$$\hat{p}(\mathbf{x},\omega) = -\frac{\omega^2 x_i x_j \, \mathrm{e}^{-\mathrm{i}\omega|\mathbf{x}|/c_0}}{4\pi c_0^2 |\mathbf{x}|^3} \widetilde{T}_{ij}\left(-\frac{\omega\mathbf{x}}{c_0|\mathbf{x}|}, \omega\right). \tag{5}$$

Eq. (5) shows that, for each value of ω and a given observer position $\mathbf{x}$, only a *single* wavenumber, $\mathbf{k} = -\omega\mathbf{x}/c_0|\mathbf{x}|$, contributes to the radiated sound. This wavenumber is directed to the observer and has magnitude $|\mathbf{k}| = |\omega\mathbf{x}/c_0|\mathbf{x}|| = \omega/c_0$.

For propagation to an observer at an angle θ to the jet axis, these spectral components travel in the axial direction with speed $c_0/\cos\theta$, i.e., supersonically. When the jet speed is such that the eddy convection velocity is subsonic, almost all components of the turbulence are silent. For example, all frozen turbulence satisfying Taylor's hypothesis and hence being a function of $\mathbf{x} - t\mathbf{U}_c$ only, generates no noise when its convection velocity $\mathbf{U}_c$ is subsonic: the most energetic elements of the turbulence then have no influence on the far-field sound. This is illustrated in Fig. 1, where the elements that generate sound that travels in the direction θ have an axial phase speed $\omega/k_x = -c_0/\cos\theta$, whereas the most energetic elements in the turbulence convect with speed $\omega/k_x = -U_c$. If we plot contours of $\widetilde{T}_{ij}(\mathbf{k},\omega)$ as shown in Fig. 2, the peak amplitude aligns with the direction $\omega/k_x = -U_c$. But, it is only the very weak supersonic components that influence the far-field sound. Taking all angles of propagation θ into account, the sound producing components form a very thin cone in $c_0|\mathbf{k}| \leqslant \omega$. It is only the turbulent fluctuations in this cone that we are interested in for sound generation – all other components are irrelevant, even though their amplitudes are much larger they are uncoupled to the far-field.

Some of the large-scale structures in a jet flow approximate to instability waves, so it is instructive to see how disturbances in a wave packet generate far-field sound. We will consider a disturbance whose amplitude A slowly evolves as it convects downstream. We can illustrate these effects through a two-dimensional example in which the pressure perturbation is given on the plane $y = 0$ to be

$$p'(x,0,t) = A(\varepsilon x)\, \mathrm{e}^{\mathrm{i}\omega(t-x/U_c)} \quad \text{with } \varepsilon \ll 1 \text{ and } M_c = U_c/c \ll 1 \tag{6}$$

as illustrated in Fig. 3. We wish to find the solution to the wave equation $\partial^2 p'/\partial x^2 + \partial^2 p'/\partial y^2 = (1/c^2)\partial^2 p'/\partial t^2$ in $y > 0$. The function $A(\varepsilon x)$ might be, for example, a Gaussian and for definiteness we take $A(\varepsilon x) = \varepsilon\, \mathrm{e}^{-\varepsilon^2 x^2}$.

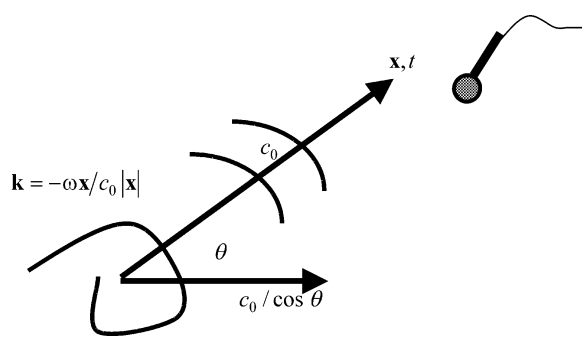

Fig. 1. Sound radiation in direction θ.

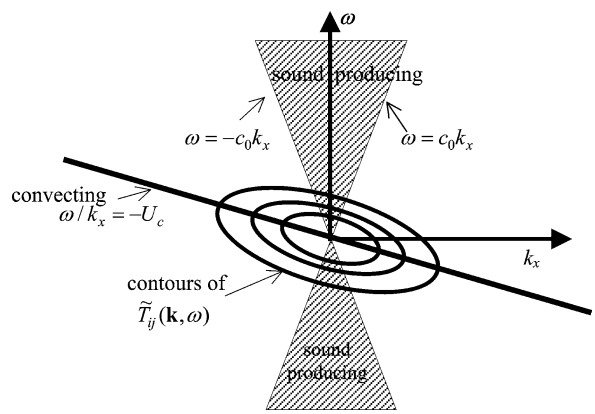

Fig. 2. Only wavenumber-frequency components with $\mathbf{k} = -\omega\mathbf{x}/c_0|\mathbf{x}|$ generate far-field sound.

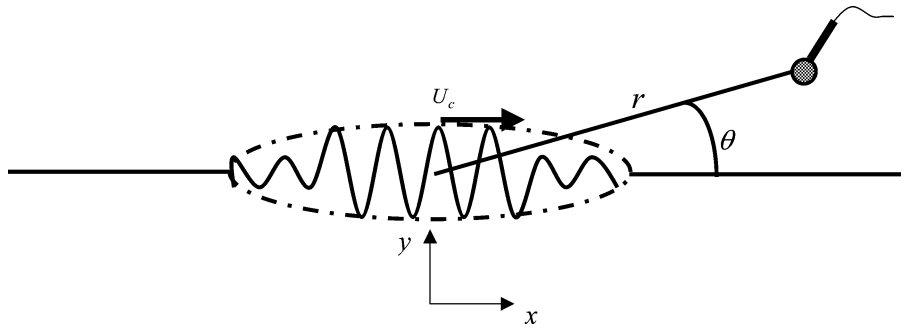

Fig. 3. A convecting and evolving wave packet.

The solution to the wave equation in $y > 0$ can be conveniently expressed in terms of an integral over wavenumber, and for **x** in the far-field the integral can be evaluated by the method of stationary phase [6] to give

$$p'(x, y, t) = \sqrt{\frac{1}{2r\kappa}}\, \mathrm{e}^{\mathrm{i}\omega(t-r/c)+\mathrm{i}\pi/4} \sin\theta \exp\left[\frac{-\kappa^2}{4M_c^2\varepsilon^2}(1 - M_c\cos\theta)^2\right], \tag{7}$$

where $\kappa = \omega/c_0$. The sound pressure decays with the inverse square-root of distance in this two-dimensional problem, but the most striking aspect of the form in Eq. (7) is that the pressure field is exponentially small when M_c is subsonic. (Note the factor $\exp[\frac{-\kappa^2}{4M_c^2\varepsilon^2}(1 - M_c\cos\theta)^2]$ in Eq. (7).) If the wave packet were to convect without change it would be silent. It only generates sound through its slow modulation in amplitude $A(\varepsilon x)$. For subsonic flows, the pressure field is largest near $\theta = 0$ and decays exponentially fast away from that direction. This type of behaviour was first discovered by Crighton and Huerre [6] who called it 'super-directive'. The far-field sound is so weak that an extensive source length contributes to it and, as is typical for a large source, leads to a highly directional sound field.

Although this example is highly idealised, many aspects remain true in general. In particular, the subsonically convected large-scale flow structures do not generate sound directly, but only through their gradual change in amplitude, and that sound is beamed into directions near the jet.

3. Numerical solutions

Figs. 4 and 5 show the results of Freund [7] from a Direct Numerical Simulation (DNS) of a jet of Reynolds number 3600 (based on jet diameter), $M_j = 0.9$. In this calculation, the 'near-field' numerical simulation was extended to determine the flow on a 'Kirchhoff' surface, that is a surface sufficiently far outside the jet that the flow perturbations there are linear. The sound radiated to the far field can be determined directly from the unsteady flow on this surface either by evaluating an integral over the surface, or through a spectral solution of the wave equation outside the surface. We see that the DNS agrees well with the experimental data obtained by Stromberg et al. [8] at the same low Reynolds number. Through comparison with other data at more practical Reynolds numbers, we see that, although the peak sound radiation near $\theta = 30°$ which is generated by the large-scale structures is correctly recovered, there is a real Reynolds number dependence of the sound field at $\theta = 90°$. This is not surprising: the sound radiated in this direction is produced by small-scale turbulence, which is Reynolds number dependent.

These results were obtained using the numerical solution to determine the flow on a Kirchhoff surface and then integrating over this surface to calculate the far-field sound. While this is an effective way of determining the far-field sound from near-field information, the pressure perturbations on the Kirchhoff surface are influenced by all the sources and so this gives no information about the locations of the most significant sources. To overcome that Freund [7] used the numerical solution to investigate the statistics of $S(\mathbf{x}, t) = \partial^2 T_{ij}/\partial x_i \partial x_j$. Fig. 6 shows contours of $\widehat{S}(k_x, \omega)$, the cross power-spectral density of $S(\mathbf{x}, t)$, integrated over r and θ. The contours approximate to the elongated ellipses sketched in Fig. 2. The peak phase velocity, or coherent 'eddy convection velocity', can be deduced from the slope of the major axis of the ellipses and is found to be $\omega/k_x = -c_0/3$, i.e., $M_c = 0.3$, corresponding to one-third of the jet-exit speed. As we noted in Section 2, these intense spectral elements with subsonic phase speed are silent: it is only turbulent fluctuations within the sonic cone that radiate sound. Another view of that is shown in Fig. 7, which is a plot of the cross-power spectral density at a particular value of frequency. It is only part of the decaying 'tail' of the turbulent spectrum that contributes to the sound field. While many numerical calculations may resolve the spectral peak, great care is needed to ensure that the weaker noise-producing components are not contaminated by extraneous noise sources. DNS calculations, carefully carried out, provide insight into the turbulent acoustic sources and are a tremendous resource against which to evaluate models (see for example Freund and Colonius [11]). However, they are only

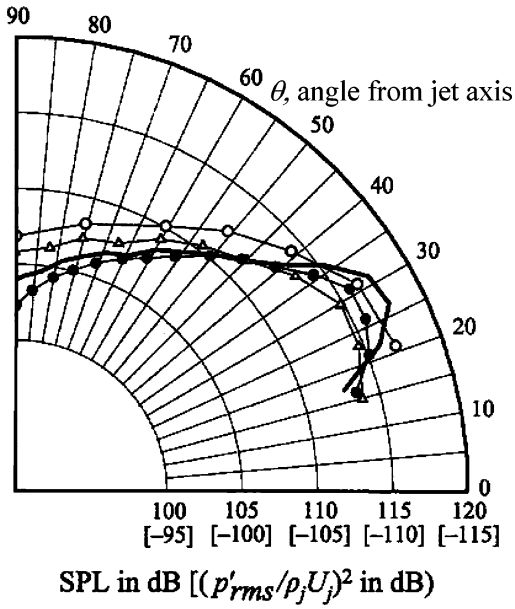

Fig. 4. Directivity predicted using DNS solution for the flow on a 'Kirchhoff' surface and a spectral solution for the far-field sound, — DNS, Re 3600 [7], experimental data, • Re 3600 [8], ∘ Re 2×10^5 [9], △ Re 6×10^5 [10] (from [7]).

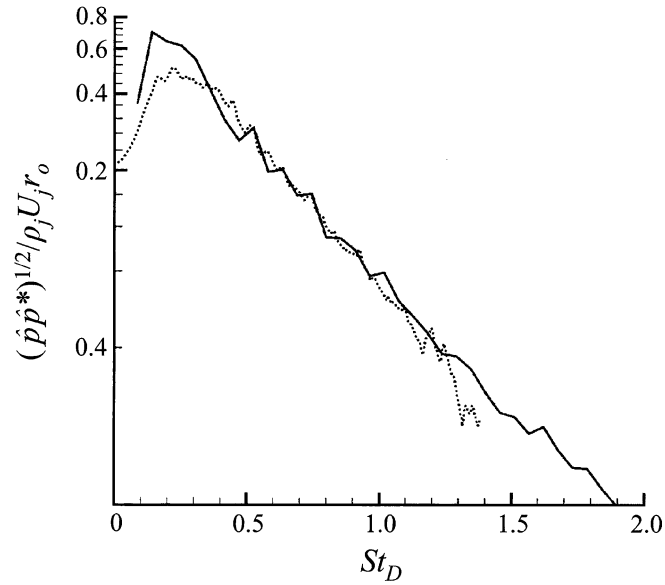

Fig. 5. Far-field pressure spectrum at $\theta = 30°$ for Re = 3600, — DNS calculation Freund [7], ····· experimental data Stromberg et al. [8] from Freund [7].

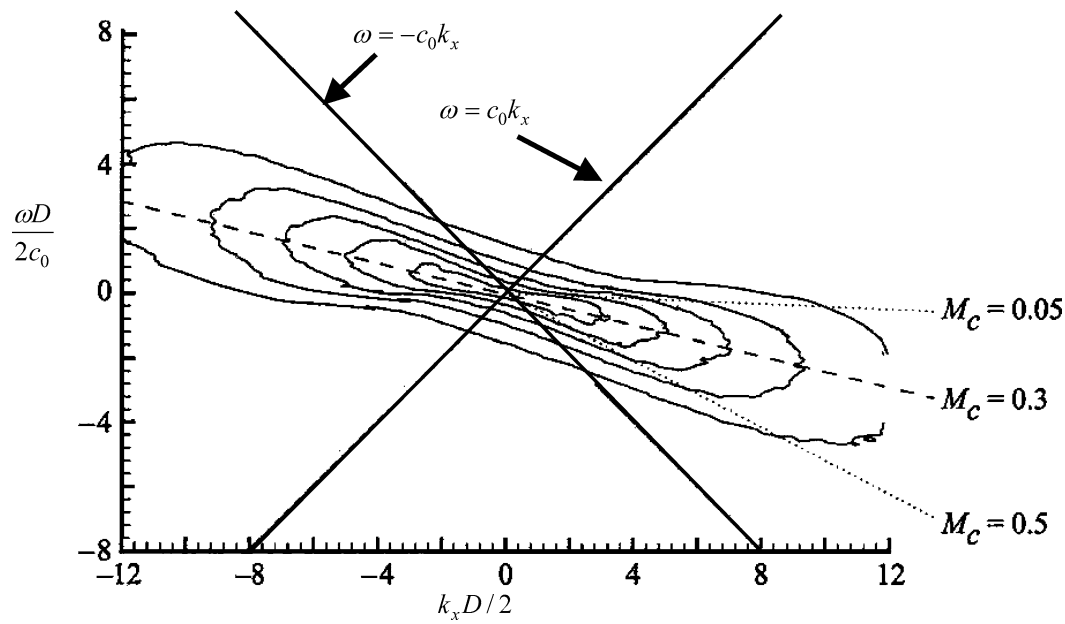

Fig. 6. Contours of cross power-spectral density $\widehat{S}(k_x, \omega)$ from Freund [7].

feasible at low Reynolds numbers. For the higher Reynolds numbers of more practical interest at least some of the sound sources have to be modelled.

Large Eddy Simulation (LES) is able to give reasonable predictions for the low frequency sound (Choi et al. [12], Bogey et al. [13], Seror et al. [14], Zhao et al. [15], Rembold et al. [16]). But as shown in Rembold et al. [16] in Fig. 8, the high-frequency sound is under-predicted. The length-scales associated with such high frequency sound are prohibitively short and

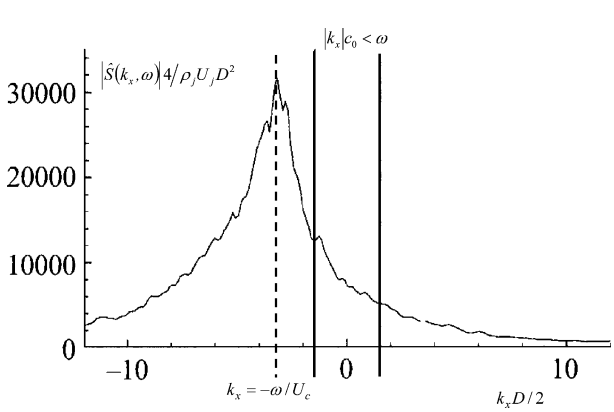

Fig. 7. Axial wavenumber spectrum at frequency $\omega = 3c_0/D$ in a Re = 3600 jet from Freund [7].

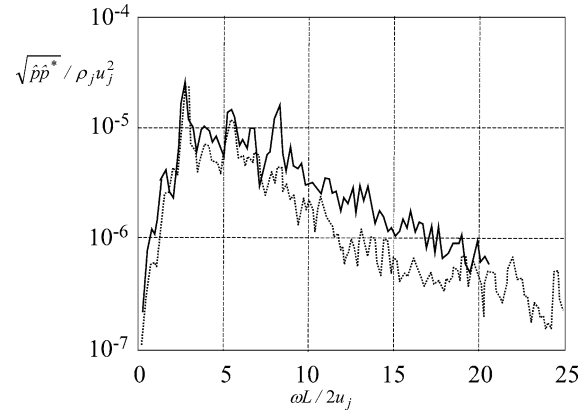

Fig. 8. Calculated far-field spectra at 30° to the jet axis for a 5:1 low Reynolds number rectangular jet of Mach number 0.5. L = major axis length. DNS —, LES ····· (after Rembold [16] from a combination of their Figs. 6(b) and 10(b)).

are not resolved by the LES. It is necessary to model these sources and determine their contributions to the far-field sound. So when LES is used to provide the information about the jet flow, the statistics of the high frequency/short-length scale acoustic sources must be modelled. (It is worth noting that, since these depend on multi-point correlations, the unresolved length-scales tend to be somewhat larger than the LES grid-scale.) If a steady Reynolds-Averaged Navier–Stokes (RANS) solution is used to determine the jet flow, then models are needed for all the acoustic turbulent sources. So for either LES or RANS calculations, one needs to model at least some turbulence fluctuations that are important acoustic sources and determine their contribution to the far-field sound. This can be done through an acoustic analogy.

4. Acoustic analogies

The idea of an acoustic analogy is to express the exact equations of motion in terms of linear fluctuations from a base flow, which describes the propagation effects, and nonlinear fluctuations, which are viewed as the acoustic source terms. Different base flows have been used [17]. The Lighthill equation (1) involves a base flow which is a state of rest. Ffowcs Williams [18] used a base flow of uniform motion, appropriate for turbulent sources in a moving stream. Mani [19] and Dowling et al. [20] used a 'top hat' velocity profile to account for propagation effects, that is a base flow in which there is a jet of uniformly moving air in an otherwise stationary flow. Of course real jets have a continuous velocity profile and Lilley [21] and Balsa and Gliebe [22] modelled the base flow as a parallel shear flow, not evolving axially. In that case the linearised fluctuations lead to the compressible Orr–Sommerfeld operator, and the nonlinear sources are complicated. For jet-like mean flow profiles, the Orr–Sommerfeld equation has eigensolutions which describe convective instabilities and grow without limit in a non-evolving parallel shear flow. These arise because the base flow has been idealised. If instead one uses the time-mean at each location **x** as the base flow, then the propagation effects are described by the linearised Euler equations and the nonlinear terms may be viewed as source terms, in the spirit of Lighthill's pioneering analogy.

To illustrate this approach we begin with the equations of conservation of mass, momentum and energy for a compressible viscous fluid motion, expressed in conservation form:

$$\frac{\partial U_i}{\partial t} + \frac{\partial F_{ij}}{\partial x_j} = 0 \quad \text{for } i = 1, \ldots, 5; \ j \text{ summed 1 to 3}, \tag{8}$$

where $\mathbf{U} = [\rho, \rho u_1, \rho u_2, \rho u_3, E]^{\mathrm{T}}$, $F_{1j} = \rho u_j$, $F_{ij} = \rho u_i u_j + p\delta_{ij} - \sigma_{ij}$, for $i = 2, \ldots, 4$, and $F_{5j} = u_j(E+p) - u_i\sigma_{ij} - \lambda\partial T/\partial x_j$, E is the total energy per unit volume, $E = \rho(e + \frac{1}{2}(u_1^2 + u_2^2 + u_3^2))$ and σ_{ij} is the viscous stress tensor, λ the thermal conductivity and e the internal energy. The ideal gas law relates the pressure, temperature (internal energy) and fluid density. The flow at each position **x** is then decomposed into its time-mean and a time-varying part, using density-weighted decomposition as usual in compressible flow. Thus for the momentum flux we write: $\overline{\rho}\overline{\mathbf{u}} = \overline{\rho}\tilde{\mathbf{u}}$, $\mathbf{u}(\mathbf{x}, t) = \tilde{\mathbf{u}}(\mathbf{x}) + \mathbf{u}'(\mathbf{x}, t)$. The time mean of Eq. (8) then leads to the usual Favre-averaged Navier–Stokes equations for the mean flow, with a closure model required for the time mean of the nonlinear terms (the density-weighted Reynolds stresses and turbulent energy flux). The equations for the time-varying elements can then be determined by subtracting from Eq. (8) its time mean. In our approach, we rearrange the

resulting equations, retaining all the terms that depend linearly on the unsteady flow on the left-hand side of the equation, with all other terms treated as right hand side source terms. These can be expressed symbolically as

$$L_{ij}V'_j = N'_i, \quad \text{where } \mathbf{V} = [\rho', v'_1, v'_2, v'_3, p']^{\mathrm{T}} \text{ and } \mathbf{v}' = \rho\mathbf{u}'/\bar{\rho}. \tag{9}$$

L_{ij} is the operator for the linearised Euler equations, involving the mean flow variables and partial derivatives with respect to $\mathbf{x}$ and t, and the energy equation has been reformulated to provide an equation for the time-varying pressure. The 'source' term $\mathbf{N}'$ involves terms which are either non-linear in the unsteady flow or time-varying viscous terms. The choice of Favre-averaging ensures that the time-mean of $\mathbf{v}'$ is zero and that $N'_1 = 0$. Moreover, for $i = 2, \ldots, 4$, $N'_i = -\partial R'_{ij}/\partial x_j$, where $R'_{ij} = \rho u'_i u'_j - o'_{ij} - \overline{\rho u'_i u'_j}$. The source term in the energy equation, N'_5, is small for an isothermal jet but may be significant when the jet is hot.

At least some of the elements of R'_{ij} will have to be modelled. This is particularly important in directions whose angles are greater than 60° from the jet axis because in these directions it is the small-scale elements of the turbulence that generate sound [23]. Bechara et al. [24,25] and Bailly and Juve [26] use what they call a stochastic noise generation and radiation model to construct a random source in the time domain with known spectral properties. They express the time mean turbulent velocity at position $\mathbf{x}$, $\mathbf{u}_t(\mathbf{x})$, as a sum of wavenumber components, whose amplitude $\hat{u}_n(k_n)$ is chosen to match the von Karman–Pao turbulent kinetic energy wavenumber spectrum and whose phase ψ_n is random. They take

$$\mathbf{u}_t(\mathbf{x}) = \sum_{n=1}^{N} \mathbf{i}_n \hat{u}_n(k_n) \cos(\mathbf{k}_n \cdot \mathbf{x} + \psi_n), \tag{10}$$

which is extended into the time domain using the local mean convection velocity $\mathbf{U}_c$ and a Gaussian distribution of frequencies about $u'k_n$, where u' is the rms turbulence velocity fluctuation:

$$\mathbf{u}_t(\mathbf{x}, t) = \sum_{n=1}^{N} \mathbf{i}_n \hat{u}_n(k_n) \cos\big(\mathbf{k}_n \cdot (\mathbf{x} - \mathbf{U}_c t) + \psi_n + \omega_n t\big). \tag{11}$$

They then solve the linearised Euler equations in the time domain with this source term.

However, since the source depends on the turbulent fluctuations, it is the statistics of the source that can be modelled, not its time history. It is therefore somewhat artificial to construct a time history. An alternative approach is to manipulate the linearised Euler equations, so that they need only the statistics of the turbulent sources, by making use of an adjoint Green function, $\mathbf{G}$.

We choose $\mathbf{G}$ to satisfy the partial differential equation, $L^*_{ij}G_i = -S_j$ where L^*_{ij} is the adjoint operator of L_{ij} and $\mathbf{S}$ is a source distribution that we can specify. After some algebra, Eq. (9) leads to

$$\int V'_j S_j \,\mathrm{d}^3\mathbf{x}\,\mathrm{d}t = \int \left(R'_{ij} \frac{\partial G_i}{\partial x_j} + G_5 N_5 \right) \mathrm{d}^3\mathbf{x}\,\mathrm{d}t. \tag{12}$$

The left-hand side of Eq. (12) gives information about the field variable $\mathbf{V}'$, weighted by our choice of the source $\mathbf{S}$ in the adjoint problem. For example, if we choose $S_5 = \delta(\mathbf{x} - \mathbf{X})\delta(t - T)$, with $\mathbf{X}$ far away from the jet, and all other components of $\mathbf{S}$ zero (this is equivalent to choosing a point sink at $(\mathbf{X}, T)$ in the energy equation of the adjoint linearised Euler system), then the left-hand side of (12) simplifies to $p'(\mathbf{X}, T)$ and we have an equation giving the distant pressure perturbation as equal to the right-hand side of (12). In the spirit of Lighthill's and Lilley's equations, this involves an integral of an acoustic source with a Green function. Here the acoustic source depends nonlinearly on the velocity fluctuation, and all the effects of the sound propagating through the evolving jet are described by the vector Green function $\mathbf{G}$ of the linearised Euler equations. With the choice: $S_5 = \delta(\mathbf{x} - \mathbf{X})\,\mathrm{e}^{-\mathrm{i}\omega t}$ the left-hand side of Eq. (12) reduces to $\tilde{p}(\mathbf{X}, \omega)$, the Fourier transform of the pressure perturbation and the right-hand side just involves $\widetilde{\mathbf{G}}(\mathbf{x} \mid \mathbf{X})$, the Fourier transform of $\mathbf{G}$. The power spectral density of the distant pressure $\widetilde{P}(\mathbf{X}, \omega)$ can be determined from this in the usual way (see, for example, Crighton et al. [27]) and for an isothermal jet, is given by

$$\widetilde{P}(\mathbf{X}, \omega) = \int \mathcal{R}_{ijkl}(\mathbf{x}, \boldsymbol{\Delta}, \omega) \frac{\partial \widetilde{G}_i}{\partial x_j}(\mathbf{x} \mid \mathbf{X}) \frac{\partial \widetilde{G}_k}{\partial x_l}(\mathbf{x} + \boldsymbol{\Delta} \mid \mathbf{X})\, \mathrm{d}^3\mathbf{x}\, \mathrm{d}^3\boldsymbol{\Delta}, \tag{13}$$

where $\mathcal{R}_{ijkl}(\mathbf{x}, \boldsymbol{\Delta}, \omega)$ is the cross-correlation of the turbulent sources,

$$\mathcal{R}_{ijkl}(\mathbf{x}, \boldsymbol{\Delta}, \omega) = \int \overline{R'_{ij}(\mathbf{x}, t) R'_{kl}(\mathbf{x} + \boldsymbol{\Delta}, t + \tau)}\, \mathrm{e}^{-\mathrm{i}\omega\tau}\, \mathrm{d}\tau.$$

Eq. (13) gives the far-field spectral density in a particularly convenient form: the right-hand side involves the statistics of the turbulent field and a vector Green function which is a solution of the harmonic adjoint linearised Euler equations; a simple system of equations, whose solution we can find numerically to a high accuracy.

There are several advantages to this approach. It is convenient to calculate **G** in the frequency domain. Moreover, if we wish to find the radiated sound averaged over the azimuthal direction and the mean flow is axisymmetric, then we have an axisymmetric problem for **G** even if the turbulence itself does not satisfy axisymmetry. Simply through inspection of **G** we can find which the source locations are most effectively coupled to the far-field sound. This would enable us, for example, to highlight the scattering effects of the jet lip or of a pylon.

It remains to decide how to scale $\mathcal{R}_{ijkl}(\mathbf{x}, \boldsymbol{\Delta}, \omega)$, the statistics of the fluctuating Reynolds stress. Tam and Auriault [23] have produced some of the most effective scaling of turbulent sources. However, their approach is hard to follow, starting as it does from an analogy with the kinetic theory of gases. In our notation their assumptions are equivalent to

(i) a parallel mean flow,
(ii) R'_{ij} isotropic, i.e., $R'_{ij} = q_s\delta_{ij}$ with a particular simple form for the cross-correlation of D_1q_s/Dt, where $D_1/Dt = \partial/\partial t + \bar{u}\partial/\partial x_1$ and $\bar{u}$ is the local mean axial velocity.

Specifically, Tam and Auriault take

$$\overline{\frac{D_1q_s}{Dt}(\mathbf{x},t)\frac{D_1q_s}{Dt}(\mathbf{x}+\Delta,t+\tau)} = \frac{Q_s^2}{\tau_s^2}\exp\left[-\frac{|\Delta_x|}{\bar{u}\tau_s} - \frac{\ln 2}{\ell_s^2}\left((\Delta_x-\bar{u}\tau)^2+\Delta_y^2+\Delta_z^2\right)\right]. \tag{14}$$

Q_s scales on $\rho u'^2$ and Tam and Auriault relate it to the turbulent kinetic energy just as in the work of Bechara et al. [25], $Q_s = A\bar{\rho}\frac{2}{3}k$. As in Bechara et al.'s model τ_s is scaled on the dissipation time, $\tau_s = c_\tau k/\varepsilon$ and ℓ_s on the integral length-scale $\ell_s = c_l k^{3/2}/\varepsilon$, where A, c_τ and c_l are constants. Using values of the parameters $\bar{u}$, τ_s and ℓ_s obtained from a RANS calculation, Morris and Farrassat [28] show that this scaling gives excellent agreement with measured spectra (see Fig. 9). However, here we are making assumptions about D_1q_s/Dt, that would more reasonably be made about q_s, but that gives a poor fit to the experimental data (see Fig. 10). The linearised Euler equations with exact source terms provide a framework for analysing the implications of different source models.

We see that it is only because Tam and Auriault take R'_{ij} to be isotropic that $R'_{ij}\delta G_i/\delta x_j$ reduces to $\frac{1}{3}R'_{ii}\nabla\cdot\mathbf{G}$ and through the continuity equation for **G** to $-\frac{1}{3}R'_{ii}(\bar{\rho}\gamma)^{-1}D_1G_4/Dt$. ($G_4$ is the 'density-like' variable in the adjoint Euler equations.) The convective time derivative acting on G_4 leads to an extra factor ω which has been cancelled by the assumed form of D_1q_s/Dt. If instead the jet is not assumed to be isotropic then ω is replaced by $\mathrm{d}\bar{u}/\mathrm{d}y$ leading to a source with cross-correlations of the form given by Eq. (14). This is an area of active research. There is other good evidence that the isotropic condition should be relaxed [30].

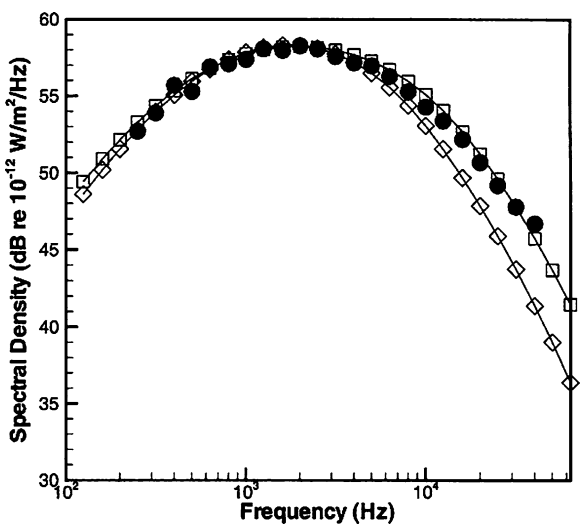

Fig. 9. Power spectral density of the far-field sound at 90° to the jet axis predicted using the source statistics in Eq. (14) (from [28]). ◇ Tam and Auriault's [23] parameters, □ Morris and Farassat's [28] parameters, ● experiment, Tanna et al. [29].

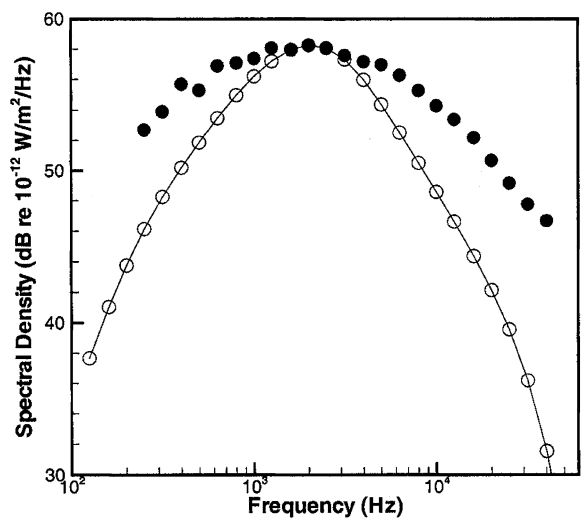

Fig. 10. Power spectral density of the far-field sound at 90° to the jet axis predicted by modelling the cross-correlation of $q_s(\mathbf{x},t)$ by a Gaussian (from [28]). ○ scaling the cross-correlation of q_s by a Gaussian, ● experiment, Tanna et al. [29].

5. Conclusions

Jet noise remains challenging because of the wide range of frequencies and wavenumbers, and because the sources of sound are very weak. The most energetic components of the turbulent field do not generate sound, it is only those elements with supersonic phase speeds that couple to the radiated far-field. DNS is a very useful tool to identify source mechanisms but at the Reynolds numbers of practical interest some of the turbulent structures that are sources of sound must be modelled. Sound from the large-scale structures dominate near the jet at angles θ less than 60° from the jet axis. These can be captured by LES and this is an area of current activity. At greater angles from the jet axis much of the sound is due to small scales and these need to be modelled. Simple models for the turbulent statistics have led to good predictions for the sound from these sources. A vector Green function, which is a solution of the adjoint Euler equations, with a source at the observer's position, provides a convenient mechanism to couple the far-field sound to the source statistics.

Acknowledgements

The reciprocal theorem described in Section 4 was derived when the authors were on sabbatical leave at Caltech. The warm welcome extended by the Faculty and the support of the Gordon Moore Foundation, which made this visit possible, is gratefully acknowledged.

References

[1] M.J. Lighthill, On sound generated aerodynamically: I. General theory, Proc. Roy. Soc. London Ser. A 211 (1952) 564–581.
[2] J. Bridges, E. Envia, D. Huff, Recent developments in US engine noise reduction research, ISABE-2001-1017, 2001.
[3] D.E. Crow, A comprehensive approach to engine noise reduction technology, ISABE-2001-1011, 2001.
[4] T. Colonius, S.K. Lele, P. Moin, Boundary conditions for direct computation of aerodynamic sound generation, AIAA J. 31 (1993) 1574–1582.
[5] T. Colonius, S.K. Lele, P. Moin, Sound generation in a mixing layer, J. Fluid Mech. 330 (1997) 375–409.
[6] D.G. Crighton, P. Huerre, Shear-layer pressure fluctuations and superdirective acoustic sources, J. Fluid Mech. 220 (1990) 255–368.
[7] J.B. Freund, Noise in a low-Reynolds-number turbulent jet at Mach 0.9, J. Fluid Mech. 438 (2001) 277–305.
[8] J.L. Stromberg, D.K. McLaughlin, T.R. Troutt, Flow field and acoustic properties of a Mach number 0.9 jet at a low Reynolds number, J. Sound Vib. 72 (1980) 159–176.
[9] E. Mollo-Christensen, M.A. Kolpin, J.R. Martucelli, Experiments on jet flows and jet noise far-field spectra and directivity patterns, J. Fluid Mech. 18 (1964) 285–301.
[10] P.A. Lush, Measurements of subsonic jet noise and comparison with theory, J. Fluid Mech. 46 (1971) 477–500.
[11] J.B. Freund, T. Colonius, POD analysis of sound generation by a turbulent jet, AIAA paper 2002-0072, 2002.
[12] D. Choi, T.J. Barber, L.M. Ciappetta, M. Nishimua, Large eddy simulation of high Reynolds number jet flows, AIAA Paper 99-0230, 1999.
[13] C. Bogey, C. Bailly, D. Juve, Computation of sound radiated by a 3D jet using large eddy simulation, AIAA Paper 2000-2009, 2000.
[14] C. Seror, P. Sagaut, C. Bailly, D. Juve, On radiated noise computed by large-eddy simulation, Phys. Fluids 13 (2001) 476–487.
[15] W. Zhao, S.H. Frankel, L. Mongeau, Large eddy simulations of sound radiation from subsonic turbulent jets, AIAA J. 39 (2001) 1469–1477.
[16] B. Rembold, J.B. Freund, M. Wang, An evaluation of LES for jet noise prediction, in: Proceedings Summer Program 2002, Centre for Turbulence Research, Stanford, 2002.
[17] M.E. Goldstein, A unified approach to some recent developments in jet noise theory, Int. J. Aeroacoustics 1 (2002) 1–16.
[18] J.E. Ffowcs Williams, The noise from turbulence convected at high speed, Philos. Trans. Roy. Soc. London 255 (1963) 469–503.
[19] R. Mani, The influence of jet flow on jet noise, Parts 1 and 2, J. Fluid Mech. 73 (1976) 753–793.
[20] A.P. Dowling, J.E. Ffowcs Williams, M.E. Goldstein, Sound production in a moving stream, Philos. Trans. Roy. Soc. London Ser. A 288 (1978) 321–349.
[21] G.M. Lilley, On the noise from jets, noise mechanisms, CP-131-Agard 113.1-13.12, 1974.
[22] T.F. Balsa, P.R. Gliebe, Aerodynamics and noise of coaxial jets, AIAA J. 15 (1977) 1550–1558.
[23] C.K.W. Tam, L. Auriault, Jet mixing noise from fine-scale turbulence, AIAA J. 37 (1999) 145–153.
[24] W. Bechara, C. Bailly, P. Lafon, S.M. Candel, Stochastic approach to noise modeling for free turbulent flows, AIAA J. 32 (1994) 455–463.
[25] W. Bechara, P. Lafon, C. Bailly, S.M. Candel, Application of a $k-\varepsilon$ turbulence model to the prediction of noise for simple and coaxial free jets, J. Acoust. Soc. Am. 97 (1995) 3518–3531.
[26] C. Bailly, D. Juve, A stochastic approach to computing subsonic noise using linearised Euler equations, AIAA 99-1872, 1999.
[27] D.G. Crighton, A.P. Dowling, J.E. Ffowcs Williams, M. Heckl, F.E. Leppington, Modern Methods in Anaytical Acoustics, Springer-Verlag, 1992.
[28] P.J. Morris, F. Farassat, Acoustic analogy and alternate theories for jet noise prediction, AIAA J. 40 (2002) 671–680.

[29] H.K. Tanna, P.D. Dean, R.H. Burrin, The Generation and Radiation of Supersonic Jet Noise. Vol. III, Turbulent Mixing Noise Data. AFAPL-TR-76-65-Vol 3, Wright-Patterson AFB, OH, 1976.
[30] A. Khavaran, Role of anisotropy in turbulent mixing noise, AIAA J. 37 (1999) 832–841.